Russian Chemical Reviews **78** (4) 375 – 386 (2009) © 2009 Russian Academy of Sciences and Turpion Ltd

DOI 10.1070/RC2009v078n04ABEH003897

Stereolithography fabrication and characterization of syntactic foams containing hollow glass microspheres

T Roques-Carmes, Ph Marchal, A Gigante, S Corbel

Contents

I.	Introduction	375
II.	Stereolithography principle	376
III.	Syntactic foams used in stereolithography	377
IV.	Properties of syntactic foams based on hollow glass microspheres	379
V.	Stereolithography fabrication of syntactic foam samples	382
VI.	Conclusion	385

Abstract. This review presents the stereolithography fabrication of epoxy and acrylate syntactic foams based on hollow glass microspheres. Physicochemical analysis has been performed on the fabricated 3D syntactic foam items containing different amounts of microspheres. The surface free energies, light transmittance, density of the syntactic foams were investigated. Criteria for the choice of a polymeric binder are discussed. The bibliography includes 48 references.

I. Introduction

Syntactic foams are special type of composite foam materials in which hollow rigid microspheres are dispersed in a solid polymer binder.[1] The voids within the microspheres lower the density of the foam, the rigid walls increase stiffness while the polymeric phase provides structure to the foam. Syntactic foams are advantageous for applications that require materials with high impact strength, low thermal conductivities, high specific compressive strength, and high thermal stability.[2] Syntactic foams composed of an epoxy resin matrix and low-density glass microspheres are the most studied because of their extensive applications. They are used, in particular, for the construction of boats and deep-water submarines.[3,4] They have also been successfully used in electronic industries[5] and weight sensitive aerospace industries.[6] In addition, they are used as the core material for the structural sandwich composites in military aviation applications.[7]

The nature of the polymer matrix binder, depending upon its chemical class, governs the fabrication process and also performance of the foam. Polymer resins, particularly, epoxies and acrylate resins, are used in fabrication of syntactic foams. To produce the syntactic foam samples, the resin is generally injected under pressure into a mould filled with hollow glass microspheres.[8] Such process hinders manufacturing of complicated geometry items and thus limits the range of applications of syntactic foams. In this context, application of these materials in stereolithography fabrication of complex shapes seems promising.

Stereolithography is a rapid prototyping method for three-dimensional polymer part fabrication by a stepwise growth process.[9–12] The method is based on laser-induced photopolymerisation process where liquid resin exposed to laser radiation is layer-by-layer converted to solid polymer.[13]

The advantages of stereolithography are its flexibility in manufacturing solid objects of different geometries and dimensions, its accuracy and manufacturing efficiency.[14]

Stereolithography has been successfully used in fabrication of complicated shapes of various ceramic and metal-based composite materials that are dispersions of corresponding powders [silica, silicon nitride, alumina, hydroxyapatite, (zirconate titanate oxides PZT), aluminium and copper] in photocurable liquid medium.[15–25] Acrylate or epoxy resins are the most often used liquid photocurable media. It is to be noted that thorough tuning of photocurable composition is necessary to ensure the homogeneity and the target properties of the solid polymer.

Until recently, stereolithography was not used in syntactic foam production. The challenge was to extend the stereolithography method to the direct fabrication of items of these materials with good mechanical properties.

This review describes the first application of stereolithography method in producing articles of syntactic foams of two types on the base of hollow glass microspheres dispersed in epoxy or acrylate resin. Main physicochemical

T Roques-Carmes, Ph Marchal, A Gigante, S Corbel Nancy-Université 1, Département de Chimie Physique des Réactions (UMR 7630 CNRS-INPL), Centre de Génie Chimique des Milieux Rhéologiquement Complexes, Rue Grandville 1, BP 20451, 54001 Nancy Cedex, France. Fax (33-0383) 37 81 20, tel. (33-0383) 37 53 35, e-mail: thibault.roques-carmes@ensic.inpl-nancy.fr (T Roques-Carmes), tel. (33-0383) 17 50 10, e-mail: philippe.marchal@ensic.inpl-nancy.fr (Ph Marchal), tel. (33-0383) 17 51 11, e-mail:alexandra.gigante@ensic.inpl-nancy.fr (A Gigante), tel. (33-0383) 17 51 14, e-mail: serge.corbel@ensic.inpl-nancy.fr (S Corbel)

Received 1 September 2008
Uspekhi Khimii **78** (4) 402 – 415 (2009)

and mechanical properties of these syntactic foams are studied, namely, surface free energy, particle incorporation in the foam, particle repartition (light transmittance), porosity and sample deformation.

II. Stereolithography principle

Application of stereolithography method for production of 3D articles from polymers by means of layer-by-layer formation (growth) under the action of laser radiation started recently, in the 1980s (first laser stereolithography apparatus was issued by 3D-Systems in 1988).

Stereolithography process of article production implies two steps. At the first srep, the 3D object is reproduced in a computer-aided-design (CAD) file (Fig. 1 *a*).[9] Then, it is numerically sliced into layers of a given thickness defining the different horizontal cross sections of the object to be manufactured (Fig. 1 *b*). The sections (layers) are like contours of a topographic map; the surface relief is approximated by steps the height of which is equal to one layer thickness.

Basing on the coordinates of contour lines or surfaces, the CAD file is obtained to calculate the laser beam trajectory, which thus reproduces the corresponding horizontal section on the surface of liquid photocurable compound.

At the second step, the article is produced by means of layer-by-layer curing of liquid photocurable compound upon laser irradiation (Nd-YAG-laser was used in syntactic foam fabrication, YAG is yttrium–aluminium garnet $Y_2Al_5O_{12}$, $\lambda = 355$ nm, pulse frequency of 20 kHz, scan rate over the surface of photocurable suspension was 0.1 to 0.8 m s^{-1}, Fig. 2 *a*). To achieve this, a platform supporting the solid part is placed inside the reactor containing the photocurable compound. The platform is immersed in the compound at a depth of one layer thickness. Then laser beam scans the liquid surface. (The photocurable mixture consists of solid particles dispersed in liquid photocurable matrix with photoinitiator added.)

Focused beam of laser UV radiation is directed by a computer. The UV radiation is absorbed by the photoinitiator which, in turn, generates free radicals or other reactive species. The latter initiate polymerization of a liquid monomer. The reactive species are formed only in the irradiated zone, so the polymerization occurs only in this zone resulting in local phase transition in the medium (liquid to solid transition).

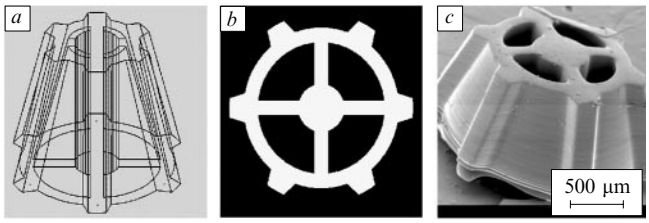


Figure 1. Main stages of stereolithography process. (*a*) Creation of digital image (CAD-file) of a 3D object; (*b*) slicing of the 3D model into horizontal layers (sections), (*c*) an article fabricated by the strereolithography process.

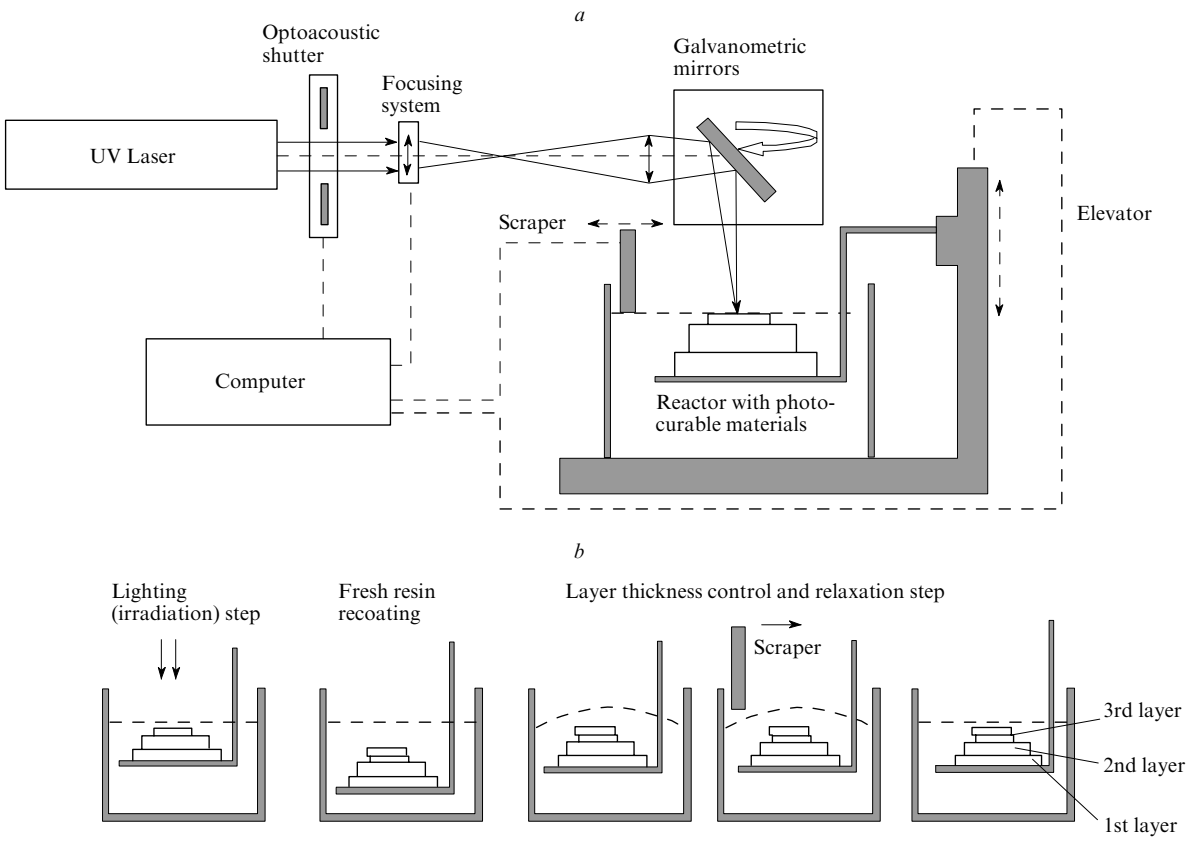


Figure 2. Scheme of the strereolithography set-up (*a*) and principle of a part layer-by-layer fabrication (sequence of layer stacking) (*b*).

As laser beam proceeds over the trajectory calculated for the first layer, the solid layer is formed corresponding to the first section of the object. After that, deposition of a subsequent layer of photocurable resin on the already polymerized part continues the manufacturing process.

For this purpose, after the exposure step, the platform is completely immersed in the reactive medium and then moved upwards, such that between the last cured layer and the resin surface there is a new layer of fresh resin (Fig. 2 *b*). This is accomplished by a precision motor driven elevator. During this step of layer recoating it is necessary to wait until the resin surface becomes completely flat and level in order to have accurate thickness control.

This procedure is repeated until the polymer solid part is built. The stacking of the layers leads to the three-dimensional physical part. After a few hours, the platform is raised and the completed part removed (Fig. 1 *c*).

Resolution (accuracy) of the process is defined by the film thickness, the kinetics of photopolymerization [10] and particle diffusion. Typical layer thickness is 200 μm. Thinner layers increase the production time which is undesirable taking into account potential creaming of the dispersion. On the other hand, thicker layer may require longer laser exposure and thus also longer production times.[26] The maximum part size is limited by the size of the monomer bath, typically 30 litres. The dimensions of the photoreactor are related to the product size: from millimetre range sizes to larger 20 cm^3 objects. Typical dimensions are about $250 \times 250 \times 250$ mm (SLA-250 apparatus). Parts of such a size typically take about 20 h to form.

Novel techniques of stereolithographic growth of 3D objects have been developed recently, for example, liquid-crystal mask-based techniques,[16, 17] DMD mask-based techniques (Digital Micro-mirror Dynamic Mask),[27] two-photons absorption microfabrication processes.[28]

III. Syntactic foams used in stereolithography

Homogeneous, stable and well dispersed suspensions are prerequisites for stereolithography fabrication. A candidate stereolithography suspension must satisfy several requirements:

1. A high volume loading of particles is required to give dense and high quality articles. It is also mandatory to use stable particle dispersions during the fabrication process.

2. The suspension viscosity should be less than 5 Pa s in order to ensure satisfactory layer recoating and to reduce the time necessary to obtain a horizontal fresh layer completely flat.[25, 29] Generally, the highly loaded suspensions are quite viscous,[15] then thorough tuning of the composition is required. A resin of high viscosity (above 5 Pa s) flows slowly down from the top of the build platform resulting in longer time of recoating and formation of convex on the surface. If the viscosity is too high, the resin surface never becomes completely flat by gravity alone.[30] Such a suspension behaves as a paste rather than as a liquid, and conventional free-surface STL apparatus cannot be used in this case.[31] Thus viscosity of 5 Pa s is the optimum resin viscosity in conventional stereolithography with scraper to ensure a satisfactory layer recoating.

The previous free-surface STL apparatuses could not be used effectively for the film recoating and thickness control. By transposition of the tape casting process, a precision blade technique was developed to spread the suspension into a uniform layer to controlled thickness ranging from several microns to 50 μm. The layer thickness is defined by the distance between the scraper and the resin surface. The movement of the scraper is synchronized with the other operations and its speed is adapted to the rheology of the liquid.

3. The suspension must be curable with required depth and resolution. The curing depth (C_d, or cured layer thickness) must be high enough to avoid an excessive time of fabrication. The adjunction of particles greatly modifies the behaviour of the resin under photopolymerization due to the scattering and absorption of the incident light beam by the particles.[32] Two parameters characterize the reactivity of an STL resin and define the photosensitivity of UV curable resin, these are the effective penetration depth of the resin (D_p) and critical exposure of the resin at the laser wavelength (E_c).[12] The theoretical expression of the curing depth, C_d, is derived from the Beer–Lambert law of absorption and can be written as [10]

$$C_d = D_p \ln\left(\frac{E}{E_c}\right), \tag{1}$$

where E is the laser exposure on the resin. The critical exposure parameter, E_c, is the laser energy below which the polymerization does not occur. A good resin for STL is characterized by low values of E_c to allow starting the reaction with low energy dose, and high values of D_p in order to maximize the cured thickness. In the presence of scattering particles, the penetration depth is expressed as [30]

$$Dp = \frac{2}{3}\left(\frac{\langle d \rangle}{f_p Q}\right)\left(\frac{n_0}{\Delta n}\right)^2, \tag{2}$$

where $\langle d \rangle$ is the mean particle size, f_p is the volume fraction of particles in the suspension, Q is the scattering efficiency term, n_0 is the refractive index of the monomer solution, Δn is the refractive index difference between the particles and the monomer solution.

1. Photocurable suspensions formulation

Syntactic foams were obtained from Scotchlite glass microspheres (supplied by 3M), hollow microscopic spheres composed of water insoluble, chemically stable soda lime borosilicate glass, and two commercial resins which are standard in stereolithography process: an epoxy resin Accura SI30 (supplied by 3D systems) and 1,6-hexanediol diacrylate, HDDA (supplied by UCB). The surface of the microspheres used is smooth enough to be used with no surface pretreatment. Particle diameter is about 60 μm, wall thickness is about 2 μm, density is 0.63 g cm^{-3}, the softening temperature was measured to be 980 °C. In all cases, surfactant (dispersing agent) was added to the photocurable compound to protect the particle surfaces from sticking and ensure homogeneity, stability and low viscosity of the suspension. Phosphoric ester (Beycostat C213, CECA) was used as a surfactant.[15, 33] (It was found that this dispersing agent, acting by both electrostatic and steric repulsion, efficiently dispersed the silica particles in the low polar organic media.[15])

Liquid photocurable compounds were prepared as follows. The hollow glass microspheres were first desagglomerated and coated with surfactant by ball milling in a mixture of acetone and ethanol (60 : 40 v/v) containing 1.5 wt.% of surfactant with respect to the powder. (This surfactant concentration was found to give rise to the best

state of desagglomeration of the powder and also to the lowest viscosity.) The solvent was then completely evaporated at 50 °C for 12 h. This low temperature allowed the surfactant to remain adsorbed on the particle surface. After drying, the powder was sifted through a 80 μm sieve. Finally, glass particles (with surfactant grafted on the surface) was added to the resin containing photoinitiator. The suspension was mixed during 60 min by ball milling. This procedure allowed breaking the agglomerates formed during solvent evaporation ensuring a good homogeneity.

For HDDA resin, 4 wt.% of radical photoinitiator (Irgacure 819 supplied by Ciba Specialty Chemicals) was added to accelerate the resin photopolymerization under UV laser irradiation. Free radical process transformed the monomer into linear polymer with low cross-linked density. Using the expertise through our previous work,[34–36] the SI30 resin was polymerized with the help of a cationic photoinitiator. In this case, the 3D network was developed that restricted the mobility of polymer segments.

2. Properties of photocurable suspensions

The study of the rheological behaviour of the STL suspensions is essential in view of the features of layer-by-layer article fabrication from hollow glass microsphere suspensions in epoxy or arcylate resin with the use of a scraper. Shear thickening behaviour of the suspension is detrimental for the spreading of the resin layers with the scraper. During this spreading, the suspension is subject to a shear having the shear rate ($\dot{\gamma}$) evaluated as

$$\dot{\gamma} = \frac{S}{h},$$

where S is the scraper rate, h is the thickness of the deposited resin layer. Shear rate in a steady state regime is defined as

$$\tau = \eta\dot{\gamma},$$

where τ is the stress, and $\eta = \eta(\dot{\gamma})$ is sample viscosity. To avoid thickening, the scraper rate is adjusted so that required viscosity and shear rate are achieved.

Another parameter to be taken into account when selecting the STL suspensions is their stability against creaming. The particle creaming should be consistent with the fabrication rate to avoid a progressive increase in glass microsphere content of the syntactic foam. The creaming period for the suspension of hollow glass microspheres in the resin is determined visually, while the fabrication time, after the time consumed for fabrication of a single layer with the required curing depth. The latter was measured upon production of a one-layer part by one scanning of the laser beam. The profile depth of a polymerized line was measured by optical profilometry system (UBM system). The laser exposure on the resin surface, E, was expressed by

$$E = \frac{2P_0}{\pi w_0 v_s}, \tag{3}$$

where P_0 is the power at the surface of the deposited layer, w_0 is the beam radius, and v_s is the laser scanning speed.

To determine the microsphere content within the syntactic foam, thermogravimetric analysis was used. Upon fabrication process, the organic phase can be removed by appropriate thermal treatment (debinding).[37] Thermogravimetric analyses were carried out to determine the optimum temperature for debinding. The ratio of the weight of dry hollow glass microspheres after debinding to the total weight of the syntactic foam was used to express the incorporation of glass particles.

The total light transmittance of the solid syntactic foams at a wavelength range from 300 to 800 nm was measured using a transmittance spectrometer (V-570 type, Nihon Bunko Corp., Tokyo) with an integrating sphere attachment (Model ISN-470, Nihon Bunko Corp., Tokyo). The samples were not polished before the transmittance measurements since this process might damage the glass spheres or pull them out of the resin.

The relationship between the light transmittance and the particle incorporation in the composite was also addressed using a three-dimensional model.[38] This model considers that the hollow glass spherical particles are uniformly distributed in the matrix. The radius of each particle is considered much larger than the wavelength of light ($R_p \gg \lambda$), and the refractive index difference between the particle and the matrix in the composite is quite small ($n_p^c \approx n_m^c$). The light transmittance of the composite for monochromatic light with wavelength λ can be calculated using the geometrical shadow concept.[38] The light losses caused by travelling through the pure epoxy and the glass particle are neglected. The light transmittance is assumed to be governed only by the light scattering at the matrix/particle interface. The light transmittance of the composite, at monochromatic wavelength ($I_c = I_s/I_m$, where I_s is the light transmittance of the syntactic foam, I_m is the light transmittance of the pure epoxy matrix) is given by[38]

$$I_c = \exp(-N\pi R_p^2 h\, Q_{ext}(\rho)), \tag{4}$$

where N is is the number of particles per unit volume, R_p is the average particle radius, h is the thickness of the composite specimen. $Q_{ext}(\rho)$ is the extinction function, given by[38]

$$Q_{ext}(\rho) = 2 - \frac{4}{\rho}\sin\rho + \frac{4}{\rho^2}(1-\cos\rho), \tag{5}$$

where

$$\rho = \frac{4\pi R_p}{\lambda}(n_p^c - n_m^c). \tag{6}$$

Substituting the expression $N = 3f_p/4\pi R_p^3$ (where f_p is the particle volume fraction in the composite) into Eqn (4) one has

$$Ic = \exp\left(-\frac{3f_p h}{4R_p}Q_{ext}(\rho)\right). \tag{7}$$

Basing on the Eqn (7), the volume fraction of particles in the composite can be calculated. It is shown that the calculated particle volume fraction from light transmittance agrees well with the experimental results. Since there is no simple method for visualization of the state of particle dispersion in the polymer matrix, this method was developed to obtain the distribution of glass microspheres in composite polymer matrix. To this end, transmittance was measured at different positions on the sample.

The surface free energy of the syntactic foam composites was evaluated by measuring static contact angles toward deionized water using the sessile drop method.[39]

IV. Properties of syntactic foams based on hollow glass microspheres

1. Rheological properties

The viscosity and the rheological behaviour of both the epoxy and acrylate suspensions of hollow glass microspheres were measured on a stress-controlled viscometer (CSL-100 supplied by Carri-Med). This instrument allows a simple shear deformation. The viscometer was also used to determine the possible thixotropic character of the suspensions by successive applications of loading (increasing stress) and unloading (decreasing stress) cycles. A time duration of 30 s was imposed between each stress rise or drop to determine short time thixotropy effect. Temperature regulation was ensured by a Peltier-effect plate. Each test was carried out in thermal steady-state.

Loading and unloading cycles had revealed the weak thixotropic feature of the samples. Loading and unloading curves were superposed, even where a delay of 30 s was imposed between stress rises and drops. Thixotropy was neglected in the following experiments.

Figure 3 *a* shows the rheological characteristics (flow, viscosity) of hollow glass microsphere/SI30 suspensions. All the curves are very similar in shape. Obviously, the steady state apparent viscosity does not vary with the shear rate. This corresponds to a Newtonian behaviour of the fluid.

In the case of the glass/HDDA suspensions, the rheological behaviour is different. Figure 3 *b* shows that shear rate affects the viscosity. At low shear rate, there is an increase in the viscosity, while almost no changes in the viscosity are observed at a high shear rate. This is indication of a shear thickening behaviour of the suspensions glass/HDDA. The particle concentration does not change the shape of the rheograms. However, curves of shear thickening behaviour shift to lower shear rates with the particle concentration.

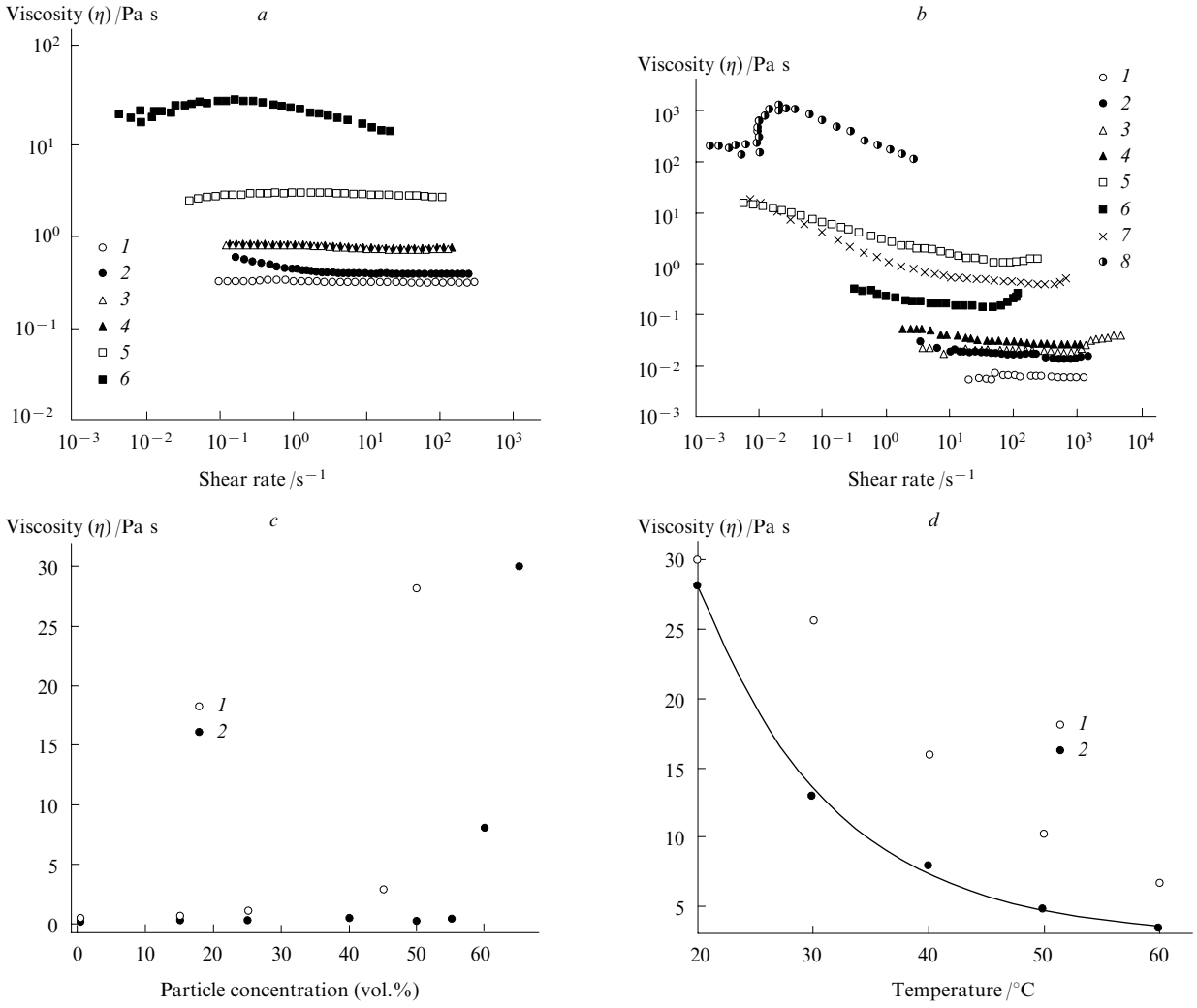


Figure 3. Rheological behaviour of suspensions.
(*a*) Flow curves of glass/SI30 suspensions differing in particle concentration [particle content (vol.%): (*1*) 0, (*2*) 15, (*3*) 25, (*4*) 30, (*5*) 45, (*6*) 50]; (*b*) flow curves of glass/HDDA suspensions differing in particle concentration [particle content (vol.%): (*1*) 0, (*2*) 15, (*3*) 25, (*4*) 40, (*5*) 50, (*6*) 55, (*7*) 60, (*8*) 65]; (*c*) suspension viscosity as a function of glass microsphere concentration for suspensions of glass microspheres in SI30 (*1*) and HDDA (*2*) resins ($\dot{\gamma} = 120\ s^{-1}$, 20 °C); (*d*) viscosity of 65 vol.% glass particles suspension in HDDA (*1*) and of 50 vol.% glass particles suspension in SI30 (*2*) as a function of temperature ($\dot{\gamma} = 120\ s^{-1}$).

The shear thickening behaviour of the suspensions is unfavourable for the spreading of the resin layers with the scraper since the usual scraper shear rate is of the same order of magnitude. To overcome thickening, the scraper speed was adjusted to obtain the desired shear rate and viscosity, using the following expression: $\dot{\gamma} = S/h$. For instance, a scraper speed of 1.2 cm s^{-1} and a layer thickness of 100 μm correspond to a shear rate of 120 s^{-1}. This was the usual shear rate of scraper processing.[15,29,34] Thus, in this paper, most of the viscosities were studied for shear rates of 120 s^{-1}. Effect of hollow glass microsphere concentration on the viscosity of suspensions in SI30 and HDDA at constant shear rate of 120 s^{-1} is shown at Fig. 3 *c*.

The viscosity of the suspension depends strongly on the resin nature. The pure resin SI30 has a viscosity 50 times higher than that of HDDA. The viscosities are 0.318 and 0.006 Pa s for the pure SI30 and HDDA resins, respectively. Consequently, the viscosity of a 50 vol.% glass microsphere suspension drops from 28.6 to 0.15 Pa s on passing from SI30 to HDDA resin. The viscosity of the suspensions increases almost exponentially with the microsphere volume fraction. The viscosity remains low for solid content between 0 and 40 vol.%. However, it undergoes a steep rise at high glass microsphere loadings (> 40 vol.% and > 55 vol.% for SI30 and HDDA, respectively). For 50 vol.% hollow glass particles suspension in SI30 and 65 vol.% hollow glass particles suspension in HDDA, the viscosity values are too high to ensure a good recoating of the layer.

To compensate the increase of viscosity the suspensions are heated.[15,33] Note that the temperature has to be lower than 75 °C to prevent thermal polymerization. As expected, rising temperature leads to a sharp decrease in the suspension viscosity. Temperature *vs*. viscosity graph is given at Fig. 3 *d*. At 60 °C, the viscosities of the 50 vol.% glass/SI30 suspension and 65 vol.% glass/HDDA suspension drop to 3.12 and 6.74 Pa s, respectively. These viscosity values are acceptable for stereolithography processing. Thus, a heating system thermostated reactor was incorporated to the stereolithography apparatus.

2. Suspension stability

Figure 4 presents the data on stability of the suspensions of hollow glass microspheres in epoxy and acrylate resins. Initially, the creamed interface height is a linear time function (Fig. 4 *a*) before reaching a plateau (due to particle compression). Similar results were obtained by other groups in studies of photocurable STL compounds.[40–43]

The slope of the initial linear part of the curve (see Fig. 4 *a*) is used to determine the creaming velocity. Fig. 4 *b* shows the experimental creaming velocity as a function of the volume fraction of particles in HDDA and SI30 resins. The creaming velocity clearly depends both on resin nature and on volume fraction of glass particles.

In SI30 the creaming velocity is roughly constant and rather low in the entire range of particle volume fractions. No significant creaming was detected during the first 5 hours. The corresponding creaming rate of 7×10^{-6} ml s^{-1} does not affect the density of syntactic foam during the STL process, since the creamed height equals 0.0252 ml after one hour of fabrication.

In contrast, in HDDA resin the creaming velocity is significantly higher and depends on the particle volume

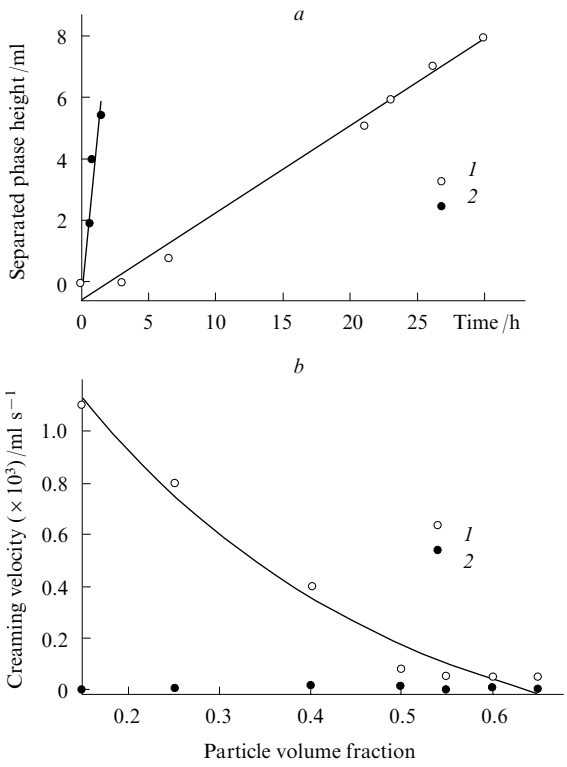


Figure 4. Suspension stability.
(*a*) Time dependence of the creaming height (the height of separated phase) for glass microsphere/HDDA suspensions with particle concentration of 50 vol.% (*1*) and 15 vol.% (*2*). The slope of the initial part of the curve was taken to determine the creaming velocity. (*b*) Creaming velocities of hollow glass particles in liquid HDDA (*1*) and SI30 (*2*) resin plotted *vs*. particle volume fraction.

fraction. The creaming trend is similar to that in the literature:[40–43] the lower the particle volume fraction, the faster the particles cream. The creaming velocity remains significant up to 40 vol.%. Creaming rates of 0.0011, 0.0008 and 0.0004 ml s^{-1} (corresponding to particle volume percentage of 15, 25 and 40, respectively) seriously affect the density of the syntactic foam during the STL process since the creamed heights are 3.96, 2.88 and 1.44 ml after one hour of fabrication. In contrast, for higher glass particle volume (over 40 vol.%) the creaming velocity becomes low. The creaming velocity of a 50 vol.% suspension is calculated to be approximately 10 times lower than that of a 15 vol.% suspension. This is in good agreement with the viscosities measured by the previous rheological experiments: the lower the viscosity, the greater the creaming velocity. In addition, in the range of high particle volume fraction no significant creaming occurs due to the existence of a sedimentation (or creaming) potential related to high steric effect between particles which hinder the creaming.[44]

It should also be noted that the creaming velocities for suspensions with dispersing agent are significantly lower than those for the bare particles. This finding confirms that a certain degree of electro-steric stabilization is still present. Redispersability studies of creamed structures give important information about the particle–particle interactions. Redispersion experiments showed that the creamed cake is easily redispersed. This indicates that the particles are not aggregated in the creamed phase.

3. Photochemical suspension reactivity

We found the polymerized depth to increase with exposure which is consistent with previous observations [12, 17, 35] of linear dependence of curing depth on the logarithm of UV exposure. This is in good agreement with the numerical model [see Eqn (1)]. Basing on Eqn (1) it is possible to evaluate the penetration depth (D_p) and the critical exposure (E_c) required to initiate the photopolymerization process. The actual penetration depth D_p is represented by the slope of the experimental plot (Fig. 5 *a*) while E_c is obtained by experimental plot extrapolation to intercept with the axis x. The observed values of the critical exposure (0.028 J cm^{-2} for HDDA, 0.035 J cm^{-2} for SI30) are independent of glass microsphere concentration in the photocurable suspension and depend only on the photoinitiator/monomer system. At the same time, the glass particle concentration significantly affects the radiation penetration depth in these resins (Fig. 5 *b*): the D_p value decreases almost linearly with the particle concentration. A remarkable feature is that all curves tend to follow a unique master curve, independent of the resin nature, indicating that the resin plays no role. Moreover, the D_p values in the cases of SI30 and HDDA are rather close. This suggests that the mechanism governing the penetration depth is only the light scattering by the hollow glass microspheres.

As the particle concentration increases, the light scattering effects become stronger and the incident photons are more likely to be scattered into the surrounding area. Consequently, fewer photons can penetrate deeper leading to a diminution of D_p. The results obtained are consistent with the previous results for silica, aluminium, silicon nitride or alumina powders suspended in polymer matrices.[15, 35] Figure 5 *c* shows that the penetration depth is inversely proportional to the glass particle volume fraction (f_p).

$$D_p \propto \frac{1}{f_p}.$$

This is in total agreement with the relation (2). At high particle volume fraction, while the curing depth is attenuated (C_d = 100 μm, D_p = 40 μm), it remains sufficient for STL applications.

Satisfactory curing depths could be achieved for filled polymer compositions but at the expense of exposure energies about 100 times higher than those of unfilled resins, with a consequent proportional expected increase in build time. This does not imply the very delicate processing of spreading of thin layers (20 – 10 μm) as previously observed with piezoelectric ceramics and metals.[19, 23] The classical STL process, which was used for polymer or

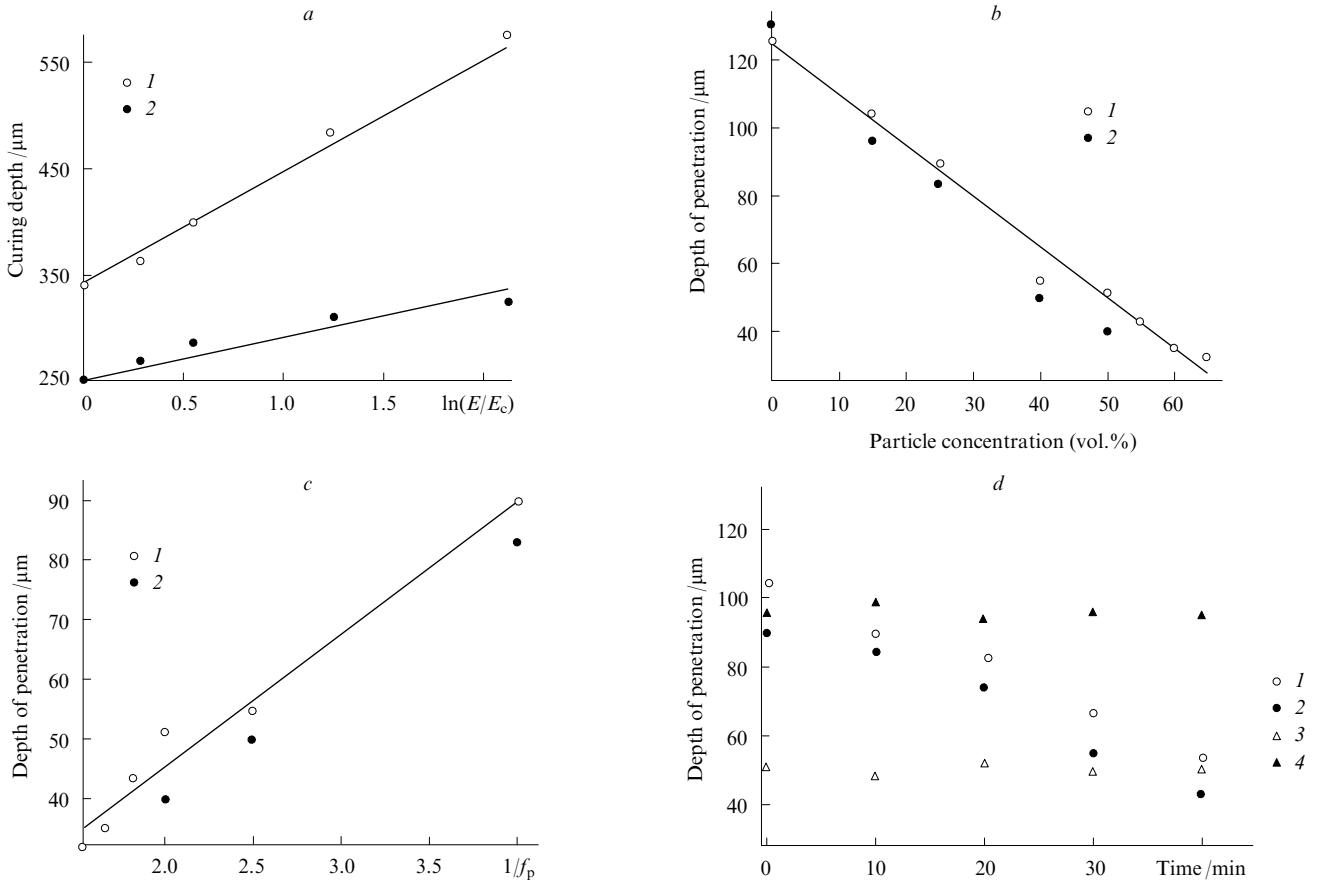


Figure 5. Photoreactivity of glass microsphere suspensions in SI30 and HDDA resin.
(*a*) Semi-logarithmic plot of curing depth for glass microsphere/SI30 suspensions [particle content 15 vol.% (*1*) and 40 vol.% (*2*)] *vs.* incident energy; (*b*) dependence of depth of penetration into hollow glass particle suspensions in HDDA (*1*) and SI30 (*2*) resin on the particle concentration; (*c*) the data of (*b*) figure replotted as the dependence of D_p on $1/f_p$; (*d*) depth of penetration as a function of delay time for different suspensions [15 vol.% glass/HDDA (*1*), 25 vol.% glass/HDDA (*2*), 50 vol.% glass/HDDA (*3*) and 15 vol.% glass/SI30 (*4*)].

alumina suspensions shaping and allows the deposition of layers ranging between 100–50 μm using a scraper, can be used.

The exposure was calculated using Eqn (3), the values $P_0 = 75$ mW and $w_0 = 250 \times 10^{-6}$ m were taken. Scan rate varied from 0.1 to 0.8 m s^{-1}.

Figure 5 *d* shows the penetration depth values for glass microsphere/resin suspensions that have been measured at different delay times. (The delay is the time between the end of suspension stirring and the actual stereolithography fabrication.) It is clear that the D_p strongly depends on the suspension lifetime for unstable suspensions (15 vol.% and 25 vol.% of glass in HDDA). When 40 minutes of STL fabrication elapsed, D_p decreased from 100 to 50 μm. This is indication of an increase in the particle concentration at the air/solution interface due to creaming. On the contrary, stable suspensions (*e.g.*, 50 vol.% of glass in HDDA and 15 vol.% of glass in SI30) show a totally different behaviour. There is no actual variation of D_p with time. Recall that stability measurements have shown that no significant creaming occurred.

V. Stereolithography fabrication of syntactic foam samples

Hollow glass microsphere suspensions in epoxy (SI30) and acrylate (HDDA) resins underwent photopolymerization at ambient temperature. For each resin, 10 sheet samples with dimensions $20 \times 20 \times 0.45$ mm were made by STL process with different microsphere content (5 vol.% to 65 vol.% for HDDA, 5 vol.% to 50 vol.% for SI30). Each sheet consisted of a stack of 200 layers 100 μm thick. Upon the completion of syntactic foam fabrication, the samples were carefully rinsed with isopropyl alcohol to remove any uncured suspension.

To obtain syntactic foams with particle concentration of (5–40) vol.%, a laser with radiation power of 75 mW and an operating scanning speed of 0.46 m s^{-1} were used. For the higher glass content, the reduction of curing depth of UV irradiation forced a reduction of the scanning speed to 0.1 m s^{-1}. In the case of syntactic foams with high resin loading by hollow glass microspheres (65 vol.% for HDDA, 50 vol.% for SI30), the fabrication process was carried out at 50 °C. The use of flexible scraper was compulsory because of high viscosity of these suspensions.

The manufacturing of glass/SI30 syntactic foam was performed with and without a scraper. No significant difference was observed between the produced solid samples. The glass/HDDA syntactic foams with low particle loading were fabricated without a scraper since the suspensions exhibited a shear thickening behaviour.

The particle creaming should be consistent with the fabrication rate to avoid a progressive increase in glass microsphere content of the syntactic foam. Continuous stirring of the glass suspension in HDDA resin was considered as a possible solution to this problem. Consequently, a stirring system (magnetic stirrer) was incorporated to the STL apparatus. However, the conditions of elaboration were far from optimal since the mixing generated turbulent flow and made a convex mound on the surface of the building part. Under these conditions the resin surface never became completely flat. Nevertheless, the re-mixing generated by the motion along the *z*-axis (motor) was not sufficient to manage particle stability during the process. Experiments were then performed without stirring.

1. Particles incorporation and distribution in the syntactic foams

The microsphere content in the syntactic foam was determined by thermogravimetry method as a ratio of the dry hollow glass microspheres after debinding to the total syntactic foam weight. The weight loss commenced at approximately 280 °C, and the polymer binder was completely removed at temperature of 540 °C. The debinding was performed as a sequence of heating to 240 °C at a rate of 1 °C min^{-1}, then further heating to 550 °C at 0.2 °C min^{-1}, followed by an isothermal step of 3 hours. The maximum temperature of 550 °C was consistent with the fact that glass microspheres displayed a softening temperature of 980 °C.

Figure 6 shows the amount of hollow glass microspheres incorporated in the syntactic foams as a function of their concentration in suspensions based on SI30 and HDDA. The amount of incorporated particles increases with the particle concentration in the solution. In the ideal case, the microsphere amount incorporated in the solid layer is expected to depend linearly on the suspension microsphere concentration (*i.e.*, the amount in solution is deposited in the foam). This ideal case is represented by the straight line in Fig. 6. The experimental data for SI30 syntactic foams fall on this single line. In this case, particle incorporation is fully determined by the particle concentration in the suspension.

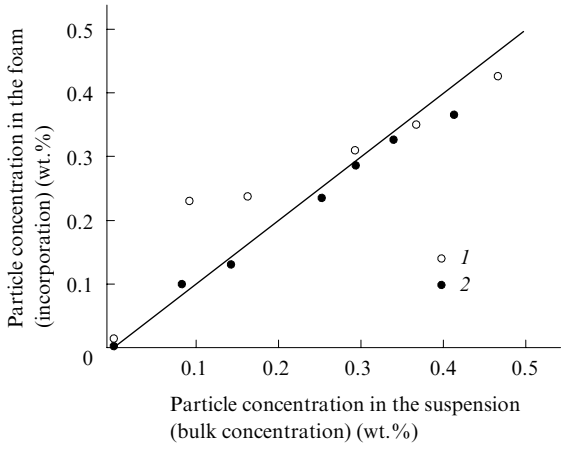


Figure 6. Amount of glass microspheres incorporated in the syntactic foams as a function of the initial bulk particle concentration in the suspensions for HDDA (*1*) and SI30 (*2*) resin. The straight line represents the ideal case for which the amount of deposited microspheres is equal to the bulk microsphere concentration in the solution.

On the contrary, for HDDA syntactic foams, the incorporation trend splits up into two principal parts. At particle concentrations in the suspension lower than 40 vol.% (read 0.3 wt.% on the abscissa axis of Fig. 6) the concentration of particles incoporated is roughly constant and significantly higher than the ideal case. This is not surprising in view of the rapid creaming of the particles in HDDA resin. This reflects the much greater number of particles at the air/solution interface than in the bulk of the suspension. This results in increased particle incorporation in the foam. It is the concentration of particles at the air/solution interface that determines their content in the composite. For glass particle volume in the suspension higher than 40 vol.%, the

amount of deposited particles increases linearly with the particle concentration in the solution. The correlation between experimental and ideal amount incorporated is almost perfect. The enhancement of the particles incorporation due to the creaming is not significant. Creaming measurements did not reveal a significant creaming behaviour (see Fig. 4 *b*).

Examples of light transmission spectra for the glass/SI30 syntactic foams are shown in Fig. 7 *a*. The light transmittance appears at wavelength above 300 nm and increases as the wavelength increases. The transmittance *vs*. wavelength plot reaches a plateau in the first part of spectrum, at wavelength 400 – 500 nm depending on the particle concentration in the suspension. In Fig. 7 *b*, the transmittance at wavelength of 800 nm for epoxy and acrylate syntactic foams is plotted against the particle volume concentration in the suspension. In the case of epoxies, the transmittance shows a gradual decrease with particle volume concentration. At particle concentrations lower than 40 vol.% the transmittance of acrylate foams is roughly constant and significantly lower than that of epoxy foams. At higher particle volume concentrations (higher than 40 vol.%) both curves show the same decrease and, moreover, a very similar transmittance.

The validity of the 3D incorporation model was verified by comparing the calculated and experimental transmittance. Conversion of the particle incorporation data to transmittance was done according to the procedure described above using Eqn (7). The incorporation data from Fig. 6 were used. Experimental transmittances and the data calculated using Eqn (7) for epoxy-based syntactic foams are given in Fig. 7 *c*. A reasonable agreement between the proposed model and experimental data is found. The agreement also suggests that the light losses in the composites are due to light scattering by the glass particles.

The model was then used to calculate the particle spatial distribution in the acrylate- and epoxy-based syntactic foams. For this purpose, the transmittance was measured at different positions on the sample (at the height of 2, 10 and 18 mm from the bottom), and particle incorporation was determined (Fig. 8). The general behaviour is very consistent with the suspension stability data presented in Fig. 4.

For SI30 syntactic foams, the particle incorporation is fairly even and does not depend on the position. The amount of particles incorporated did not change on passing from one layer to another during the fabrication. This is indication of the fact that creaming was not an issue. The slight difference in the particle distribution is about 3% – 4%, which is actually within the limit of the measurement confidence.

The particle distribution for HDDA syntactic foams produced from suspensions with particle concentrations lower than 40 vol.% is significantly broader, and it depends on layer height. The difference in the concentration of particles incorporated ranges from 20 vol.% to 40 vol.% and depends on the experimental time during the procedure. As expected, the higher the layer, the larger the incorporation (longer experiment). The particle concentration at the air/solution interface is in excess compared to that in the bulk and increases during the fabrication, thus particle incorporation increases with the number of the layer. This is not surprising in view of the high creaming velocity in HDDA suspension. As a consequence, the particle content can be hardly controlled in the syntactic foam.

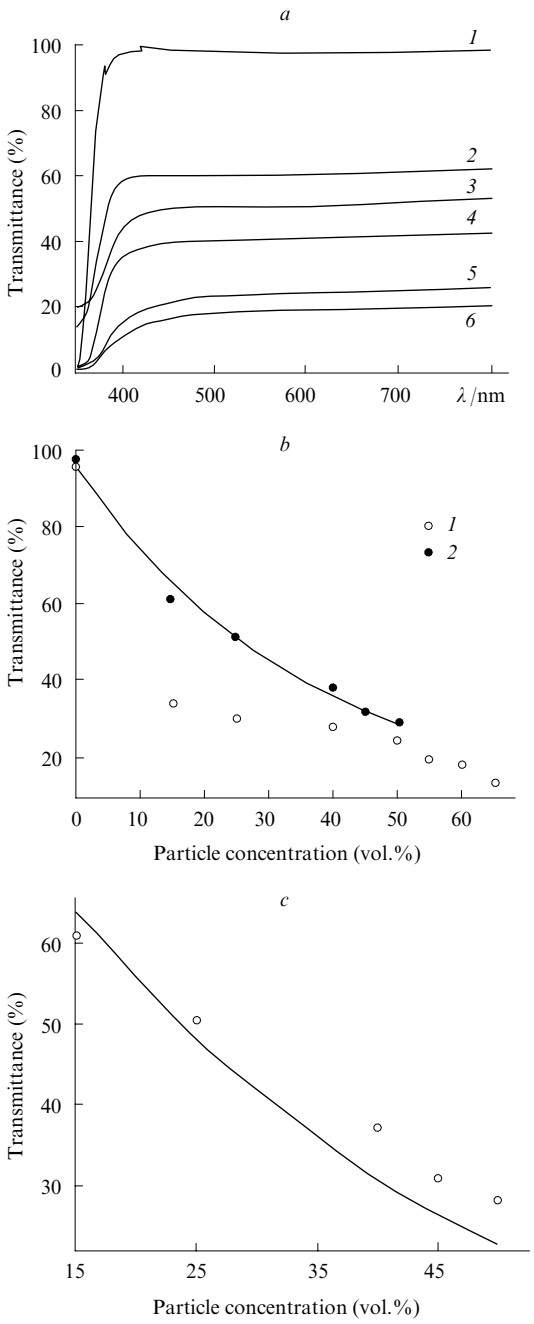


Figure 7. Light transmission of syntactic foams.
(*a*) Light transmission spectra of the glass microsphere/SI30 syntactic foams for different glass microsphere concentration in the suspension (vol.%): 0 (*1*), 15 (*2*), 25 (*3*), 40 (*4*), 45 (*5*), 50 (*6*); (*b*) plots of light transmittance at wavelength of 800 nm for acrylate (*1*) and epoxy (*2*) syntactic foams *vs*. bulk particle volume fraction in the suspension; (*c*) comparison of the experimental light transmittance (circles) of hollow glass particles/SI30 syntactic foams at 800 nm and the values calculated using Eqn (7) (represented by the solid line) (the particle incorporation values of Fig. 6 were used in calculation).

On the contrary, the incorporation does not depend on the time and the position at higher suspension particle concentration in HDDA suspensions (more than 40 vol.%), when the creaming does not occur. Note that the average of concentrations for several positions in Fig. 8 makes the result measured by thermogravimetric analysis (see Fig. 6). The concordance between the two series of data

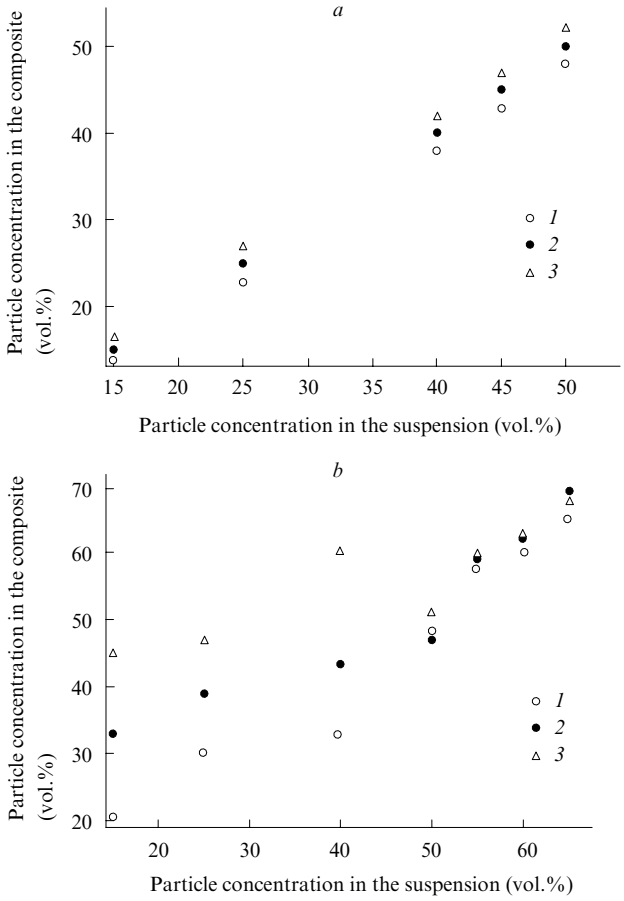


Figure 8. Spatial distribution of glass microsphere in the resin matrix as a function of particle concentration in the suspension for syntactic foams made of SI30 (*a*) and HDDA (*b*) resin.
The particle concentration in the composite is determined at height of 2 (*1*), 10 (*2*) and 18 mm (*3*), which correspond to 2, 15 amd 30 minutes of fabrication, respectively.

does also somehow validate the analytical procedures, more specifically the acknowledged difficult transmittance experiments.

2. Syntactic foam characterization

The density of the syntactic foam was measured at room temperature with a helium pycnometer (Accupyc 1330, Micromeritics Instrument, corp. Norcross, GA, USA). The density was obtained by measuring weight and volume of at least five specimens for each type of composite. Figure 9 shows the apparent density of the syntactic foams as a function of the volume fraction of microspheres in the suspension. The densities of the pure solid polymeric materials were 1.162 and 1.150 g cm^{-3} for HDDA and SI30, respectively. For epoxy syntactic foams the apparent density decreases with the volume fraction of microspheres. This is in good agreement with the published data.[8] For acrylate syntactic foams with particle concentration of 15 vol.% and 25 vol.%, the density drops remarkably. This drop cannot be attributed to experimental artifact. At higher glass content in acrylate foams, the apparent density increases with the volume fraction of microspheres.

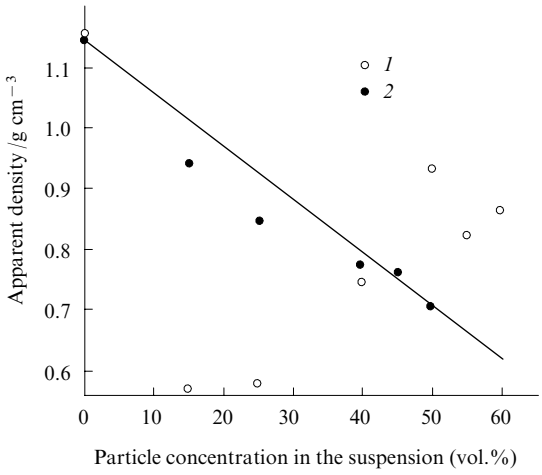


Figure 9. Apparent density of syntactic foams made of hollow glass microsphere suspensions in HDDA (*1*) and SI30 (*2*) resin as a function of particle concentration in the suspension.
The straight line represents the theoretical density calculated using Eqn (8).

A theoretical density can be calculated from a simple mixture law which considers that the syntactic foam contains only the particles and the resin (two-phase syntactic foam):

$$\rho_c = V_p\rho_p + V_m\rho_m, \tag{8}$$

where V is the volume, ρ is the density [the subscript p (particle) stands for hollow glass microspheres, m (matrix), for resin, and c, for composite]. The comparison of the theoretical (straight line) and the measured foam densities plotted *vs*. particle volume fraction is given in Fig. 9. For SI30 syntactic foams the theoretical and the experimental data follow the same trend. The theoretical predictions are consistently higher than the corresponding experimental points. The discrepancy is caused by the presence of additional voids dispersed between the matrix binder and the microspheres. We actually deal with three-phase syntactic foams composed of hollow glass microspheres, epoxy or acrylate resin and air voids acting as the third phase.[45,46] The contribution of voids in the composition of the syntactic foam was estimated by a simple difference between the theoretical and experimental densities. The concentration of voids is related to porosity as follows:

$$\phi = \frac{V_v}{V_t},$$

where V_v is the volume of void space, V_t is the total volume of syntactic foam (Table 1). The average void fraction falls in the range of 8% – 13% for SI30 syntactic foams, and 15% – 40% for HDDA foams. The largest porosities are characteristic of syntactic foams with filler fraction of 15 vol.% – 40 vol.%. This is due to the air inclusions incorporated during creaming. Samples of foams with higher particle content are free of voids (no creaming results in samples without air inclusions).

Table 1. Syntactic foam compositions.

Microsphere content in the suspension (vol.%)	Void fraction in the syntactic foam (vol.%)	
	SI30	HDDA
15	9	40
25	13	35
40	13	20
50	10	—
55	—	—
60	—	—
65	—	—

Water contact angles on the syntactic foams as a function of the particle concentration in the suspension are presented in Fig. 10. The water contact angles of HDDA and SI30 polymers without particles equal 67° and 72°, respectively. The materials composed of backbone polymers are hydrophobic in nature. The contact angles on epoxy syntactic foams decrease slightly with particle content, while the contact angles on HDDA syntactic foams unexpectedly drop to 10°. This might be caused by the accumulation of glass particles at the surface as a consequence of the creaming and/or it may more likely reflect the high porosity of the samples produced from acrylate suspensions. The surface free energy of the syntactic foams exhibit weak dependence on the content of hydrophilic microspheres.

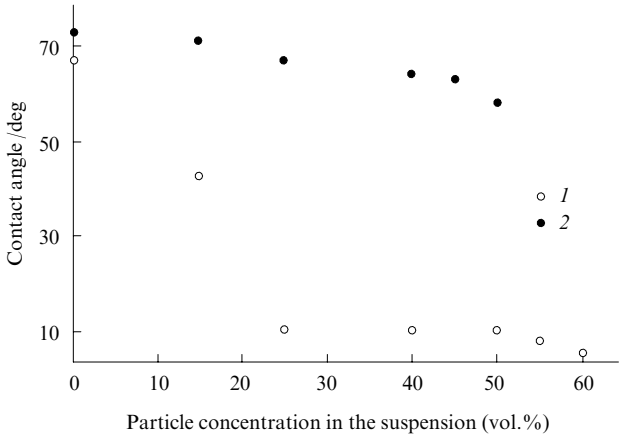


Figure 10. Water contact angle on the surface of acrylate (*1*) and epoxy (*2*) syntactic foams plotted *vs*. particle concentration in the suspension.

Photopolymerisation of the glass microsphere suspensions in SI30 and HDDA resins gave samples the dimensional stability of which (volume shrinkage) was estimated on fabricated square sheets with nominal dimensions $10 \times 10 \times 0.45$ mm and a circular hole (diameter 3.5 mm) at the centre of the sheet. The deformation of the hole is defined as the ratio of the measured diameters along the height (D_h) and along the length (D_l). This ratio D_h/D_l reflects both the longitudinal and transverse shrinkage of samples (see the measured data in Fig. 11).

This ratio would be 1 for the perfect round hole shape (no shrinkage). However ratios from 0.9 to 1.1 were considered to be within the confidence range of the measurements, which is represented by dashed lines in Fig. 11.

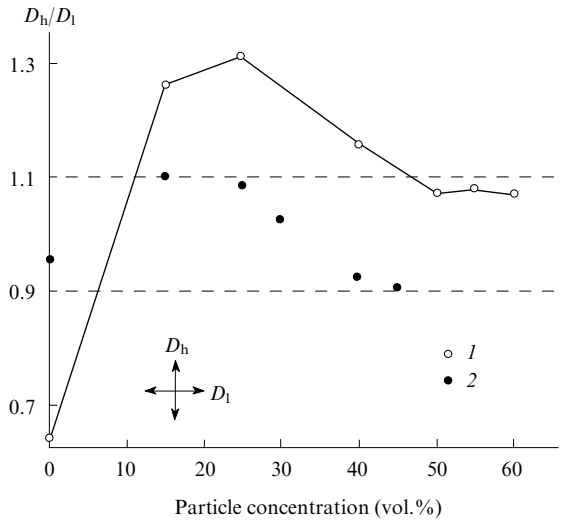


Figure 11. Dimensional stability of samples made of HDDA (*1*) and SI30 (*2*) syntactic foams as a function of the particle concentration in the suspension.
The deformation is defined as the ratio of diameters along the height (D_h) and the length (D_l) of the hole. The two dashed lines confine the range of D_h/D_l values for which no deformation was considered.

The deformation depends strongly on the resin nature. For samples made of pure SI30 resin and of the suspensions with different particle concentrations, all the data fall into the confidence range, thus indicating insignificant deformation. The cationic photopolymerization transforms SI30 monomer into a cross-linked macromolecule leading to the development of a 3D network that restricts the mobility of polymer segments and glass particles. Such resins have exceptionally low volume shrinkage resulting in good dimensional stability of the samples.[47]

In contrast, for HDDA syntactic foams a high deformation is observed for samples with particle volume fractions below 40 vol.%. Photopolymerization of pure HDDA gives high longitudinal deformation (length shrinkage). The presence of glass microspheres changes the direction of deformation, the transverse shrinkage is observed. HDDA resin is well known to suffer from high volume deformations of the polymer during the photopolymerization reaction since the photopolymerization transforms a monomer into a linear macromolecule with low cross-linked density.[48] When the glass content in the composite resin is high enough (45 vol.% – 60 vol.%), no deformation occurs. The glass microspheres displace some of the volume initially occupied by partially cured and uncured polymer. The reduced amount of the partially cured and uncured polymer results in a reduction in the shrinkage strain since the motion of segments of the macromolecules is hindered by the particles.

VI. Conclusion

Stereolithographic fabrication of syntactic foam samples consisting of hollow glass microspheres (filler) and epoxy or acrylate resin (binder) is described for the fist time. The choice of the resin for 3D sample fabrication is shown to be determined by the particle volume fraction. Epoxy resin is optimum for glass microsphere contents up to 45 vol.%. The syntactic foams obtained exhibited good spatial distri-

bution of the hollow glass microspheres in the matrix, no deformation, low surface tension and low porosity. These properties were correlated to the high stability of the suspensions due to the high viscosity of liquid resin. Higher particle volume fraction cannot be achieved during stereolithography fabrication because of the high suspension viscosity. For particle content ranging from 40 vol.% to 65 vol.%, less viscous acrylate resin is more appropriate for stereolithography. The suspensions of particles in this resin are stable due to steric potential (repulsion) between the particles hindering sedimentation (creaming). The fabricated HDDA based syntactic foams exhibited good spatial distribution of the microsphere in the matrix, no deformation, extremely low surface tension and low porosity. However, functional syntactic foam based on acrylate resin cannot be manufactured at particle volume contents lower than 45%.

The study of the rheological and photopolymerization behaviour of the hollow glass microsphere suspensions is essential for a better understanding of syntactic foams fabrication through stereolithography process. Suspension viscosity and rheological properties determine the conditions to provide the satisfactory layer recoating and the curing time. For example, glass microsphere/HDDA syntactic foams with low particle contents were fabricated without scraper, as these suspensions exhibited shear thickening behaviour which makes impossible the fresh layer flattening with a scraper.

The study on photopolymerization behaviour is necessary to select the UV curing parameters ensuring sufficient curing depth and resolution. It was possible to tune properly the suspension composition and STL process parameters in order to achieve reasonable fabrication time at a feasible cost.

References

1. K Ashida *Handbook of Plastic Foams: Types, Properties, Manufacture and Applications* (Park Ridge, NJ: Noyes Publications, 1995)
2. A Barthelemy, A R Bunsell, in *The Proceedings of the Conference of Development in Science and Technology of Composite Materials, Bordeaux, 1985* p. 349
3. F A Shutov *Adv. Polym. Sci.* **73–74** 63 (1986)
4. L Watkins, E Hershey *World Pipelines* **4** 49 (2004)
5. R C Mildner, K F Nacke, E W Veazey, P C Woodland *Modern Plastics* **47** 98 (1970)
6. M M Ashton-Patton, M M Hall, J E Shelby *J. Non-Cryst. Solids* **352** 615 (2006)
7. A Corigliano, E Rizzi, E Papa *Compos. Sci. Technol.* **60** 2169 (2000)
8. J R M d'Almeida *Compos. Sci. Technol.* **59** 2087 (1999)
9. P F Jacobs *Rapid Prototyping and Manufacturing: Fundamentals of Stereolithography* (Dearborn: Society of Manufacturing Engineers Publishers, 1992)
10. P Schaeffer, A Bertsch, S Corbel, J-Y Jézéquel, J C André *J. Photochem. Photobiol. A: Chem.* **107** 283 (1997)
11. A Y C Nee, J Y H Fuh, T Miyazawa *J. Mater. Process. Technol.* **113** 262 (2001)
12. S Zissi, A Bertsch, J-Y Jézéquel, S Corbel, D J Lougnot, J C André *Microsyst. Technol.* **2** 97 (1996)
13. Fr. P. 8411241 (1984)
14. J C André, S Corbel *Stéréophotolithographie Laser* (Paris: Polytechnica, 1994)
15. C Hinczewski, S Corbel, T Chartier *J. Eur. Ceram. Soc.* **18** 583 (1998)
16. C Provin, S Monneret *IEEE Trans. Electron. Pack. Manufacturing* **25** 59 (2002)
17. S Monneret, C Provin, H Le Gall, S Corbel *Microsyst. Technol.* **8** 368 (2002)
18. X Zhang, X N Jiang, C Sun *Sens. Actuators A, Phys.* **77** 149 (1999)
19. O Dufaud, H Le Gall, S Corbel *Trans. IChemE, A: Chem. Eng. Res. Des.* **83** 133 (2005)
20. C E Corcione, A Greco, F Montagna, A Licciulli, A Maffezzoli *J. Mater. Sci.* **40** 4899 (2005)
21. T Chartier, C Chaput, F Doreau, M Loiseau *J. Mater. Sci.* **37** 3141 (2002)
22. M L Griffith, J W Halloran *Manuf. Sci. Eng.* **2** 529 (1994)
23. A Mauzon, O Dufaud, H Le Gall, S Corbel, in *Les 10e Assises Européennes de Prototypage Rapide, Paris, 2004*
24. J W Lee, I H Lee, D W Cho *Microelectron. Eng.* **83** 1253 (2006)
25. T Chartier, C Hinczewski, S Corbel *J. Eur. Ceram. Soc.* **19** 67 (1999)
26. P Calvert, R Crockett *Chem. Mater.* **9** 650 (1997)
27. C Sun, N Fang, D M Wu, X Zhang *Sens. Actuators, A* **121** 113 (2005)
28. S Maruo, S Kawata *J. Microelectromech. Syst.* **7** 411 (1998)
29. T Chartier, M Ferrato, J F Baumard, G Coudamy *Acta Ceram.* **6** 17 (1994)
30. M L Griffith, J W Halloran *J. Am. Ceram. Soc.* **79** 2601 (1996)
31. Fr. P. 2790418-A1 (1999)
32. C Sun, X Zhang *J. Appl. Phys.* **92** 4796 (2002)
33. O Dufaud, P Marchal, S Corbel *J. Eur. Ceram. Soc.* **22** 2081 (2002)
34. M Furman, S Corbel, H Le Gall, O Zahraa, M Bouchy *Chem. Eng. Sci.* **62** 5312 (2007)
35. M Furman, S Corbel, H Le Gall, O Zahraa M Bouchy, in *Virtual Modelling and Rapid Manufacturing (Proc. 2nd Intern. Conf. on Advanced Research in Virtual and Rapid Prototyping, Leiria, Portugal)* (Ed. P J da Silva Bartolo) (Leyden: Taylor and Francis, 2005) p. 589
36. C Hinczewski, S Corbel, T Chartier *Rapid Prototyp. J.* **4** 104 (1998)
37. R K Kupka, F Bouamrane, C Cremers, S Megtert *Appl. Surf. Sci.* **164** 97 (2000)
38. Y Kagawa, H Iba, M Tanaka, H Sato, T Chang *Acta Mater.* **46** 265 (1998)
39. V Matthieu, Doctoral Thesis in Chemical Engineering, University of Nancy, Nancy, 2002
40. S A K Jeelani, G Benoist, K S Joshi, R Gunde, D Kellenberger, E J Windhab *Colloids Surf., A* **263** 379 (2005)
41. P B Laxton, J C Berg *J. Colloid Interface Sci.* **285** 152 (2005)
42. W Xu, A D Nikolov, D T Wasan *J. Colloid Interface Sci.* **197** 160 (1998)
43. D M E Thies-Weesie, A P Philipse, H N W Lekkerkerker *J. Colloid Interface Sci.* **177** 427 (1996)
44. A D Watson, G C Barker, M M Robins *J. Colloid Interface Sci.* **286** 176 (2005)
45. S Sankaran, K R Sekhar, G Raju, M N J Kumar *J. Mater Sci.* **41** 4041 (2006)
46. S J Park, F L Jin, C Lee *Mater. Sci. Eng. A* **402** 335 (2005)
47. O Dufaud, S Corbel *Chem. Eng. J.* **92** 55 (2003)
48. J Kindernay, A Blašková, J Rudá, V Jančovičová, Z Jakubícová *J. Photochem. Photobiol. A: Chem.* **151** 229 (2002)